POLITECNICO
MILANO 1863

SCUOLA DI INGEGNERIA INDUSTRIALE
E DELL'INFORMAZIONE

Executive summary

State of the art and decarbonization options for glass industry: the case of Bormioli Pharma

M.Sc. Thesis in Energy Engineering – power generation

Candidate: **Marco Cappelli**

Supervisor: **Matteo Vincenzo Rocco**

Company supervisor: **Eng. Davide Faverzani, Eng. Federico De Martino**

ACADEMIC YEAR: 2020-2021

Introduction

Bormioli Pharma is an Italian company, with headquarter in Parma, operating in the pharmaceutical packaging sector supply, specifically in the production of glass, plastic and rubber. The group counts on nine plants in three countries (Italy, Germany and France), with overall more than 1200 employees.

The glass industry belongs to the so-called *energy intensive sector* because of its great energy demand required in the melting process. Following up the initiatives of the European Union, such as the *European Green Deal*, which are meant to drive the continent towards the goal of carbon neutrality by 2050, it is necessary that governments as well as industries take up the challenge by investing in more efficient and alternative solutions in order to gradually meet the targets set by the authorities.

In this regard, this thesis work wants first to assess the state of the art of the company by exploiting the data made available over the energetic consumption along the years. Secondly, alternative technologies are discussed which can contribute to enhancing the energy efficiency of glass furnaces: *waste heat recovery*, *fuel switch* and *process optimization in combustion* are the three main fields under discussion. More specifically, heat recovery by means of thermodynamic cycles such as ORC and closed-loop JB with CO_2 have been evaluated in terms of tecno-economic performances by reporting the results achieved by researchers of the University of Padova. The last section is the core of the work: the thermodynamic model of a furnace is combined with a unit of steam reforming exploiting the thermal power of flues gasses. The analysis is enriched with the equipment sizing, their quotation and eventually the evaluation of the economic performances of the overall system by means of the Net Present Value approach, as well as a sensitivity analysis on some of the parameters and variables of the model.

1. Pharmaceutical glass industry

Two are the glass qualities that are present in the market: borosilicate and soda-lime glasses. These two are quite different: while the first offers a higher chemical inertia that makes it suitable for parenteral solutions and strong acids, the second is simpler and compatible with solid dosages and syrups. However, from an energetic viewpoint, the higher quality of borosilicate is associated with higher temperatures of the melting glass (up to 1420°C against 1350°C for soda-lime) and therefore higher heat demand. Such an outstanding amount of thermal energy is the result of the heat required to first bring the raw materials up to their melting point, to activate the endothermic reactions within the batch and lastly to heat up the melting material up to those temperature needed to achieve a good product quality. To partially reduce the energy demand, a given share of cullet (recycled glass) can be used. Because of quality concern though, such a share

is typically kept below the 50-60% in the pharmaceutical sector, whereas way higher figures can be achieved in others.

1.1. Glass furnaces classification

Glass furnaces can be classified on the basis of three different aspects. First, the **energy source**: combustion of fossil fuels (natural gas/oil) and electric approaches are the two most employed. The first is the most traditional, with heat supplied by means of radiation from flames and refractory bricks. For the second instead, heat comes from Joule effect and it is spread by means of conduction and convective motions from below the molten surface, as electric boosters are indeed submerged. Second, the **energy recovery**: exhausts gasses from fuel-based furnaces are at about 1500°C, and they can be exploited to preheat combustion air. Different approaches exist for this purpose: regenerative chambers, consisting of refractory material, operated discontinuously, able to achieve the highest recovery performance and applied to end port furnaces (air up to 1300°C). As an alternative, metallic heat exchangers in continuous mode can be used, however a lower efficiency is to be expected because waste gasses enter with a lower temperature (metallic resistance to temperature is lower than refractory bricks). This is applied on unit melter furnaces (air up to 900°C). Third aspect is on the **oxidant**: even though air is easier to be employed for combustion, it is also possible to feed pure oxygen. This leads to a lower energy demand because it avoids the heating of inert nitrogen. However, it comes with a higher cost due to oxygen supply and dedicated equipment. Moreover, a limited heat recovery capability should be expected because of the lower exhaust flow rate.

1.2. Furnaces for glass type

Based on the glass quality, different furnaces are employed by companies. In general, *borosilicate* is associated with:

- Electric furnace
- Oxy-fuel furnace
- Cyclope furnace

For *soda-lime* instead:

- Unit melter furnace
- End port furnace

The main issue for borosilicate furnaces is associated with the strong corrosion tendency of the molten glass and, most importantly, the condensation of boron components in the exhaust gasses which enhances the erosion of the furnace structure. Given that, common lifetimes of borosilicate glass furnaces are around three years.
For the case of soda-lime instead, the campaign is mainly affected by carry-over phenomena, that is dust filling the heat recovery system's channels, and the erosion of walls at the interface molten-refractories. These two are also present with borosilicate glass, but corrosion by boron components in waste gasses is way faster and more critical. For soda-lime lifetimes of eight-ten years can be expected.

2. Furnace data analysis

Within this chapter there will be presented the approach and methodology applied for the analysis of the data regarding the energetic consumption of **four** of the **Company's furnaces**. The purpose is to assess and compare their energetic performances, whose most relevant results will be presented in chapter 3. More specifically, the information available are on the operating conditions in terms of cullet, pull, electric input and natural gas feed along the furnace campaign.
The points addressed for each furnace are:

- Energy efficiency index EEI
- Heat balance
- CO_2 emission along campaign
- CO_2 emission vs electric input vs cullet

2.1. Energy efficiency index EEI

It is an index that tells how much the ageing process affects the energetic performance of the furnace. It is defined as the ratio between the actual specific energy demand and the specific energy demand when the furnace is new (EEI = 100%).

$$\mathrm{EEI} = \frac{\frac{\mathrm{kWh_{actual}}}{\mathrm{ton_{glass}}}}{\frac{\mathrm{kWh_{new}}}{\mathrm{ton_{glass}}}} \qquad [2.\ 1]$$

The index will be plotted twice. The first represents the expected trend, which is a result of historical data on past campaigns, thus playing the role of reference. The second, instead, is the actual curve computed once the energetic consumption is known.

2.2. Heat balance

By means of the heat balance, it has been possible to establish the overall heat demand of the furnace as well as each heat streams. Moreover, it was possible to determine the role of three independent and important variables in the system operating conduction: **pull, electric input** and **cullet**.
The final goal is to provide a forecast of the natural gas consumption for different furnaces when these three figures change. As for the control volume, the overall system has been considered, comprehensive of basin and heat recovery system:

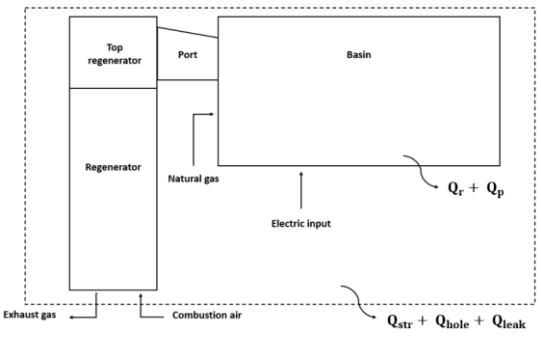

Figure 1 - Control volume heat balance

The heat balance can be written as:

$$Q_{ee} + Q_{ng} = Q_{s,l,h} + Q_{r,p} + Q_{ex} \quad [2.2]$$

The term $Q_{r,p}$ represents the sum of the net heat required by chemical reactions within the bath and the heat flux of the molten glass that leaves the chamber, whereas $Q_{s,l,h}$ accounts for the overall heat losses through the system.
While the former is a number made available by the chemical department of the Company, the latter is computed by exploiting an empirical correlation tuned on past heat balances executed by Bormioli Pharma.
Before solving the heat balance, it is possible to get the heat stored in the waste gasses Q_{ex} by exploiting a further data, which is the parameter "R" that represents the heat recovery coefficient and estimated on past balances:

$$Q_{ex}\left[\frac{kWh}{kg_{glass}}\right] = (Q_{s,l,h} + Q_{r,p} - Q_{ee})\cdot(R - 1) \quad [2.3]$$

Eventually, the Q_{ng} term is computed:

$$Q_{ng}\left[\frac{kWh}{kg_{glass}}\right] = \frac{R}{R-1}\cdot Q_{ex} \quad [2.4]$$

From which the natural gas daily volumetric demand can be obtained:

$$\dot{V}\left[\frac{sm^3}{d}\right] = \frac{Q_{ng}\left[\frac{kWh}{kg_{glass}}\right]\cdot Pull\left[\frac{kg_{glass}}{d}\right]}{LHV\left[\frac{kWh}{sm^3}\right]} \quad [2.5]$$

The role played by the independent variable cullet, pull and electric input is within the equation definitions, and therefore it was possible to establish the natural gas demand letting these three vary.

2.3. CO_2 emission along campaign

Direct carbon emissions by glass furnaces are evaluated by considering both the combustion of a fossil fuel and the carbon content of raw materials. For the first, an emission factor of 0,001984 $\left[\frac{ton\ CO_2}{sm^3}\right]$ has been applied. For the second instead, the approach consists in making use of a loss factor [1] that represents the tonne of CO_2 emitted per tonne of glass produced, being its precise value dependent on the type of glass, since the carbon content of the batch depends on the raw materials employed (borosilicate around 0,016 [tonCO2/tonPull] against 0,18 of soda-lime).

$$CO_2\left[\frac{ton}{ton_{glass}}\right] = \frac{CO_{2,ng}\left[\frac{ton\ CO_2}{month}\right] + CO_{2,rea}\left[\frac{ton\ CO_2}{month}\right]}{pull\left[\frac{ton_{glass}}{month}\right]} \quad [2.6]$$

2.4. CO_2 vs electric input vs cullet

At this point, by exploiting the data gathered with the energy balance about natural gas demand, it became possible to forecast the overall daily direct CO_2 emissions at a chosen pull[2] while letting electric input and cullet percentage vary.

3. Furnaces comparison for glass type

Within this chapter furnaces are being compared one against the others, on the basis of the data calculations obtained in chapter 2.
The discussion is structured as follows:

1. Energy efficiency index EEI
2. CO_2 emissions for different furnaces
3. Heat input Q_{tot} for different furnaces
4. Electric vs hybrid furnace: specific operating cost

3.1. Energy efficiency index

Based on the data made available by the Company, the curves have been plotted for four real furnaces along their lifetime:

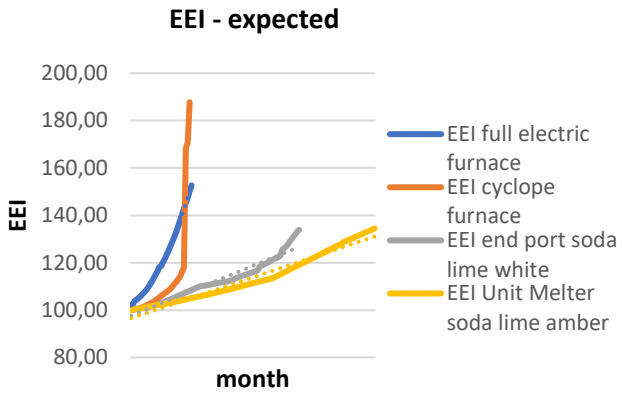

Figure 2 - Expected EEI for different furnaces

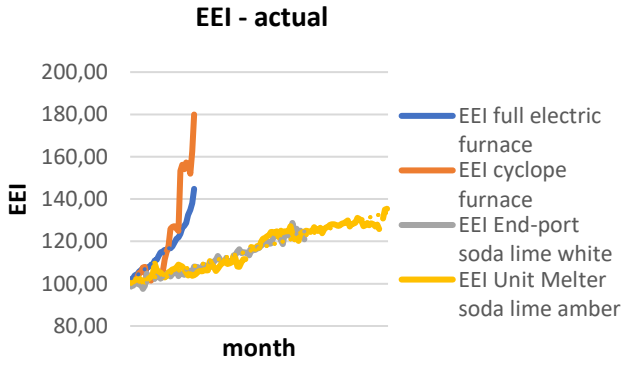

Figure 3 - Actual EEI for different furnaces

It is now immediate to notice that borosilicate glass furnaces (electric, Cyclope), despite a way shorter lifetime, exhibit a way faster worsening of the EEI. Such an expected behaviour is so extreme that soda-lime furnaces (end port, unit melter) might reach a lower EEI at the time of their disposal.

[1] Provided by the chemical department

[2] Design or average pull for the furnace

Variations from expected and actual trends are typically due to how the furnace has been conducted.

3.2. CO_2 emissions for different furnaces

According with real data from the furnaces, direct carbon emissions have been estimated for past campaigns of each. The evidence shows that Cyclope furnace has a way higher carbon intensity than end port and unit melter, mainly due to a lower pull, whereas electric furnace has only emissions due to raw materials containing carbonates, and it is basically a negligible yet not avoidable term.

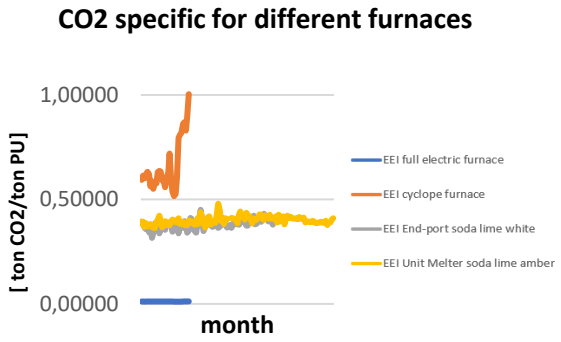

Figure 4 - specific CO2 emissions for different furnaces

3.3. Heat input Q_{tot} for different furnaces

The goal is to establish the heat input of each furnace for a given glass production, when pull is fixed at its design tonnage, as a function of **cullet** and **electric input**.
Therefore, for the borosilicate glass the electric and Cyclope furnaces are compared whereas for the soda-lime the end port and unit melter.
For a range of electric input, and exploiting the natural gas demand at the corresponding conditions obtained in section 2.2, the total heat input required has been determined as:

$$Q_{tot}\left[\frac{kWh}{kg_{glass}}\right] = \frac{\dot{V}\left[\frac{sm^3}{d}\right] \cdot LHV\left[\frac{kWh}{sm^3}\right]}{Pull\left[\frac{kg_{glass}}{d}\right]} + Q_{ee}\left[\frac{kWh}{kg_{glass}}\right] \quad [3.1]$$

Results have been tabulated and plotted. What emerges is the heat input difference between two alternative furnaces producing the same glass under fixed operating conditions.
For the case of **electric** and **Cyclope**, outcomes are reported in **Figure 5**:

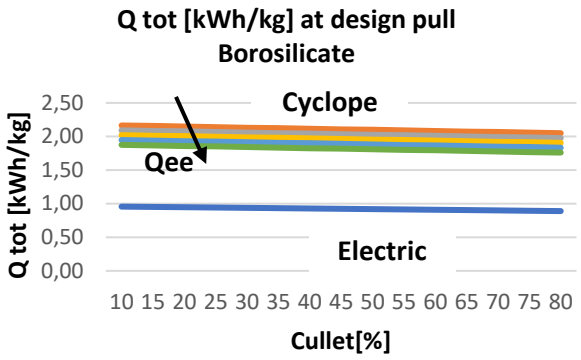

Figure 5 - total heat input for electric and Cyclope

What emerges is a significant difference between the two furnaces: full electric achieves a better heat transfer, being the electrodes submerged in the melting glass. Moreover, the absence of exhaust gases from combustion allows to avoid the loss of a great amount of energy. Therefore, it is reasonable to expect that electric furnaces allow to save a good share of energy for producing the same output
For the case of **end port** and **unit melter** instead:

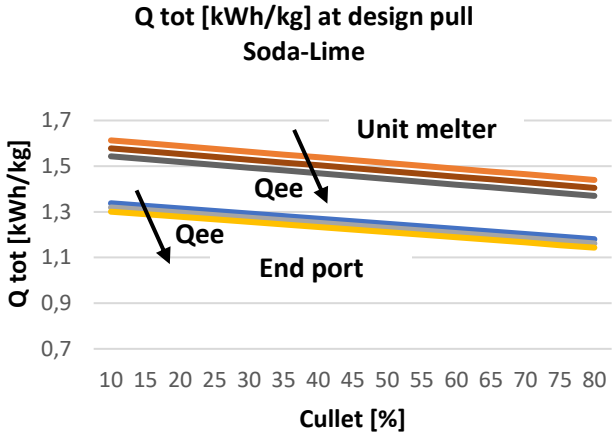

Figure 6 - total heat input for end port and unit melter

What emerges is a clear confirm of the higher thermal efficiency of the end port over the unit melter, which is to be expected being the former an enhancement of the unit melter technology. Indeed, end port furnaces achieve a greater value of heat recovery from waste gasses which in turn allows to save a not negligible amount of energy.

3.4. Electric vs hybrid: specific operating cost

Within this section it is taken into account the difference between electric and hybrid furnaces (Cyclope) in terms of specific operating cost due to energy supply and carbon emissions. The focus is to try to explain why the hybrid technology, despite being more complex in terms of structure and emissions, is still leading ahead of the full electric.
The approach is to observe the trend between 2014 – 2020, in order to justify why full electric has not yet replaced hybrid

technology in the recent past. Data regarding costs of natural gas and electricity for industrial customers are taken from ARERA [1], [2] whereas of CO_2 from SENDECO2 [3].
The method employed for the analysis is the following: once set the pull around the design value, compute the specific operating costs of energy (natural gas, electricity and carbon allowances) for each of the seven considered years, where the electric input is taken as:

- For the electric furnace, it is the overall heat input demand
- For the Cyclope, two opposite values are chosen. One is **no** electric input, while the other is **0,465 kWh/kg** (roughly 25% of the overall demand) which is basically the extreme situation as such a huge share is never really achieved in hybrid furnaces

Results are tabulated and then plotted:

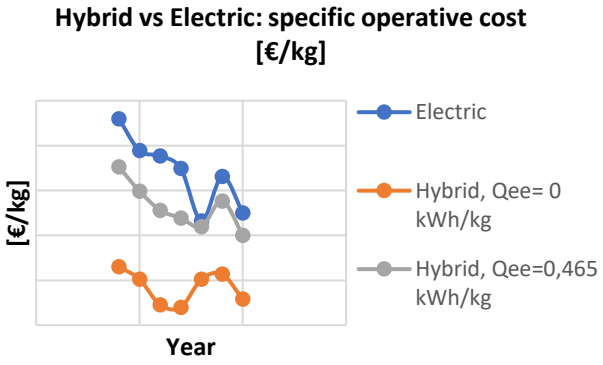

Figure 7 - specific operative cost for hybrid vs electric

What emerges is that the operating cost of full electric has been steadily above those of hybrid, despite the fluctuation in natural gas, electricity and carbon tax prices. The takeaway message is that in past years **there were not** the conditions for an overtaking of full electric on hybrid systems: from the specific costs perspective, the former have not achieved competitiveness yet.

4. Decarbonization options

Chapter 4 wants to go briefly through the most relevant technologies that can be considered for the sake of enhancing the decarbonization of the glass sector. The three area of concerns that have addressed are: *waste heat recovery, fuel substitution* and *process optimization in combustion*.

4.1. Waste heat recovery

Even though regenerative towers of end port furnaces allow to achieve up to 70% of heat recovery, flue gases leaving the regenerator are still at high temperature. However, downstream processes such as de-dusting by means of electrostatic precipitation set the lowest thermal level, as these devices are usually operated in a temperature window between 180-280 °C.

In order to enhance the waste heat recovery, a number of solutions could be implemented: *heat-to-power* and *thermo-chemical heat recovery*.
The first case is rather consolidated and consists in converting the available heat into electricity. However, to deepen this topic, please refer to chapter five.
For what concerns the second instead, it is definitely a **novel** approach and would consist in exploiting the exhaust gasses thermal content to activate endothermic reactions in order to produce an energetic vector to be burnt directly in the combustion chamber such that a reduction in natural gas consumption can be pursued. A possibility is to activate the steam reforming SMR reactions of methane to obtain syngas. This is a rather innovative configuration applied in the field, and applications in real plants are not present in literature. However, projects in this regard are under development: an example is the *Life Sugar Project*[3] [4]. According with this initiative, which is currently at the mock-up testing stage, the expected results are the achievement of a **10/15% energy consumption reduction** for glass melting and consequent carbon emissions, leading toward a more sustainable production of glass.
The thermodynamic assessment of steam methane reforming is discussed in chapter six.

4.2. Fuel substitution

With *fuel substitution* it is meant the replacement of traditional fossil fuels such as natural gas or oil with CO_2 neutral energy carriers. The main concerns are related to the unknown and unpredictable consequences on the glass quality because of the different fuel, moreover its actual availability at competitive prices as well as the lack of a widespread infrastructure are major uncertainties. The most promising choices are *biogas* and *blue/green hydrogen*.
According with [5], tests have been conducted over the co-firing option in an existing glass furnace. With an energy content from biogas up to 30%, results state that no quality issues were reported nor damages on the equipment or refractories. Even though the type of glass was not specified, it is at least reassuring that such a switch would be technically feasible and already viable with the current equipment and furnace structure. Because of limits in the supply of biogas, it would be advisable to operate with a co-firing approach which would contribute to emission reduction anyhow.
The prerequisites for the transition to hydrogen as energy carrier are mainly two. First, it must be produced with the lowest environmental impact, therefore *blue* or *green* are the choices. Second, it must become economically competitive with fossil fuels. Moreover, from a technical viewpoint, hydrogen combustion represents a challenge: higher flame temperature, different flame lengths and velocities, increased water content in flue gases. All these aspects are important to be addressed since they may play a role in the product quality, as the heat transfer properties could be different from those of natural gas, for instance. In this regard, experiments are being conducted. Among the others, the NSG Group[4] has taken on a 100% hydrogen trial for three weeks long in 2021 [6], showing up good results.

[3] Partecipants are Stara Glass, KT, Johnson Matthey, Stazione sperimentale del vetro, Università degli studi di Genova

[4] World leader architectural glass producer

However, the lack of a dedicated infrastructure together with the too little availability are still limiting factors, and most likely in the event of a transition towards hydrogen for a successful market ramp up co-firing with natural gas will be the first step, at least until the distribution grid as well as its production capacity have been developed.

4.3. Process optimization in combustion

This consists in considering expedients to better perform the combustion. In this regard, the air-fuel ratio is important, and it is suggested to seek a trade-off between energetic demand and emissions: at low ratios indeed lower NO_x are accompanied with higher CO but lower energy consumption, whereas at higher ratios higher NO_x are expected together with lower CO and greater energy expenditure. Also, the choice of the oxidizer is relevant: oxygen allows to save a large amount of fuel, even though no recovery is typically performed, but it comes with higher supply costs.
Lastly, the submerged combustion approach is proposed which has a better heat transfer and therefore efficiency. However, it poses serious issues of product quality because of a limited refining capability. This is why it is not really likely to see this technology adopted for high-quality products such as pharmaceutical field.

5. Waste heat recovery: heat to power

Chapter five is focused on the analysis of different thermodynamic cycles for heat recovery from waste gasses. Thermodynamic and economic performances of four different heat recovery systems HRSs are evaluated for either compressed air or power generation in order to determine which system is the most attractive when applied to glass furnaces. The present discussion is based on an in-depth literature research of existing papers, among which stands out the work by P. Danieli, S. Rech and A. Lazzaretto of the University of Padova "*Supercritical CO_2 and air Brayton-Joule versus ORC systems for heat recovery from glass furnaces: performance and economic evaluation*" [7] who conducted a study for two end-port glass furnaces of different sizes (small/medium) comparing alternative configurations of Joule-Brayton cycles and Organic Rankine Cycles ORC. For the sake of this work, the "small size" system is considered (150 ton/d) as it is the closest to the average operating conditions of Bormioli Pharma. The authors have also addressed the case of a bigger system, exceeding the 300 ton/d.
Four cycles have been addressed:

- Open loop, air JB cycle
- Closed loop, sCO_2 JB cycle
- Closed loop, sCO_2 JB cycle with combustion air preheating
- Organic Rankine cycle

These are hereinafter proposed in terms of process flow diagram, together with their thermodynamic operating conditions:

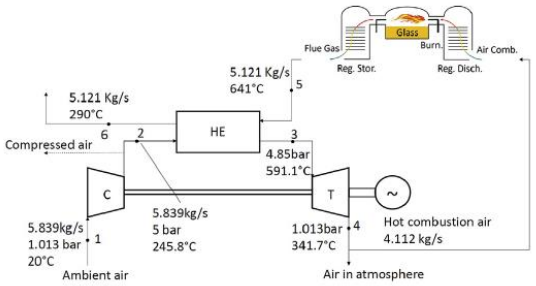

Figure 8 - Open loop, air JB cycle

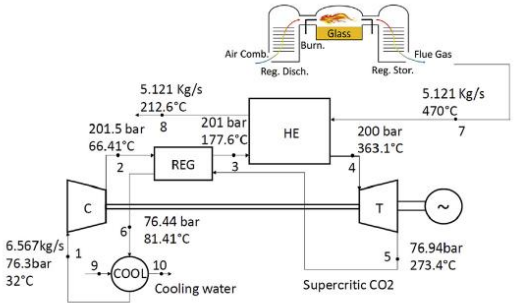

Figure 9 - Closed loop, sCO_2 JB cycle

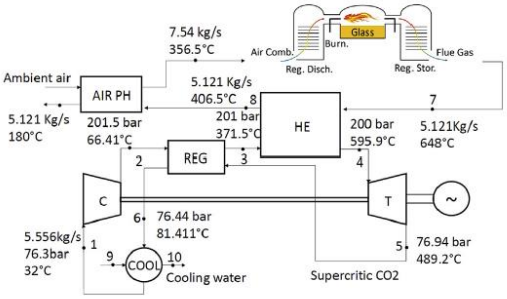

Figure 10 - Closed loop, sCO_2 JB cycle with combustion air preheating

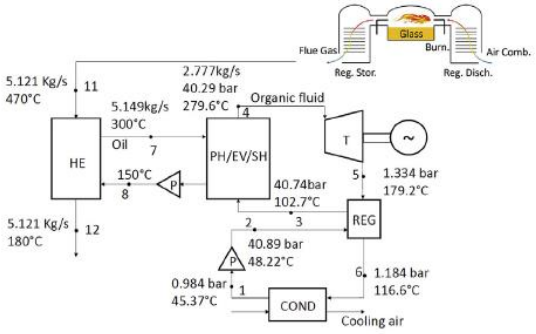

Figure 11 - ORC

The **goal** of this analysis is to assess whether alternative cycles to the well-established ORC do actually exist, both from a **power output** and **economic** point of view.
For a complete and exhaustive presentation of the methodology employed by the authors, please refer to the original paper.

In order to understand the results, let's first define the following parameters:

- Thermal efficiency of the HRS: $\boldsymbol{\eta_{th}} = \frac{\mathbf{P_{mec}}}{\mathbf{Q_{in}}}$
- Total efficiency of the HRS[5]: $\boldsymbol{\eta_{tot}} = \frac{\mathbf{P_{mec}}}{\mathbf{Q_{av}}}$
- Heat recovery coefficient[6]: $\boldsymbol{\phi} = \frac{Q_{in}}{Q_{av}} = \frac{h_{in}-h_{out}}{h_{in}-h_{out,180°C}}$
- Glass furnace + HRS thermal efficiency: $\boldsymbol{\eta_{th,furn}} = \frac{Q_{glass}+\mathbf{P_{mec}}}{m_{fuel}\cdot LHV + P_{el}}$

With h_{in}, h_{out} referred to the flue gases. Note that ϕ represents the ability of the HRS to exploit all the available thermal power of the exhaust gases, by cooling it down to 180°C, which is the lowest temperature that can be reached to avoid acid condensation in the filters. Q_{glass} is representative of the heat input absorbed by the glass.

The models obtained are evaluated in on design conditions and results are referred to the optimized case (optimization of the cycle power output)

5.1. Thermodynamic performances

The thermodynamic performances in terms of net power output and other parameters are here reported for each solution:

	Symbol	Unit	Air Brayton-Joule cycle	Standard sCO_2 cycle	sCO_2+air PH cycle	ORC
Net power output [kW]	P_{net}	[kW]	183.9	321.8	473.3	359
Working fluid mass flow rate	m_{wf}	[kg/s]	5.839	6.567	5.556	2.777
Heat source temperature	T_{gas}	[°C]	641	470	648	470
Thermal efficiency	η_{th}	[–]	0.084	0.204	0.307	0.203
Heat recovery coefficient	ϕ	[–]	0.772	0.892	0.531	1
Heat recovery efficiency	η_{rec}	[–]	0.064	0.182	0.163	0.203
Furnace + HRS thermal efficiency	$\eta_{furnace+HRS}$	[–]	0.367	0.378	0.391	0.382

Table 1 - Design performances of each HRS

What emerges is that the highest net power output extractable is 473.3 kW achieved by the *Closed loop, sCO_2 JB cycle with combustion air preheating,* against the 359kW scored by the ORC.

5.2. Economic performances

For what concerns the economic considerations, the authors have compared the four HRS in terms of ROI for both electricity and compressed air generation, separately.
Because of the uncertainty over the cost of the equipment operating with supercritical carbon dioxide (turbomachinery), the authors have addressed a minimum and a maximum cost between which the real value is supposed to be.
Results are in **Table 2**:

	ROI - compressed air [years]	ROI - compressed air + incentives [years]	ROI - electrical power [years]	ROI - electrical power + incentives [years]
Open loop, air JB cycle	9,9	8,4	10,5	8,9
Closed loop, sCO2 JB cycle (min)	8,5	7,2	8,2	6,9
Closed loop, sCO2 JB cycle (max)	9,5	8	9,2	7,8
Closed loop, sCO2 JB cycle with combustion air preheating (min)	7,3	6,1	6,9	5,9
Closed loop, sCO2 JB cycle with combustion air preheating (max)	8	6,8	7,7	6,5
ORC	7,5	6,4	7,2	6,1

Table 2 - HRS economic performances

Due to such an uncertainty the authors state that the **ORC** seems to be still the **best choice** both for the comparable ROI (between 6.1 and 7.5 years) and, most importantly, due to its high level of **readiness** and **availability** in the market even though the *Closed loop, sCO_2 JB cycle with combustion air preheating* offers interesting potential.
To conclude, *closed loop, sCO_2 JB cycle with combustion air preheating* may become a valid alternative to ORC if the cost of CO_2 turbomachines remain close to the lowest values assumed, while the innovative *Open loop, air JB cycle* and *Closed loop, sCO_2 JB cycle* are less attractive due to lower performances and high costs of the equipment which bring their ROI to uncompetitive levels.

6. Waste heat recovery: steam methane reforming

Chapter six aims at developing the thermodynamic model of an end port glass furnace with the additional presence of the steam methane reforming unit. The goal is to determine first whether this technology applied to this type of glass furnace is physically feasible and to what extent it would be possible to exploit the thermal power of the exhaust gasses in order to produce an energy vector (syngas) to be directly burnt, thus replacing a given share of energy with the synthesis gas and achieving a fuel saving as well as a carbon emissions reduction in the glass melting process, followed by the sizing of the main piece of equipment together with their quotation. This is then enriched with the economic assessment of the project by means of the Net Present Value approach. To account for different operating conditions a sensitivity analysis is also addressed: the final result allows not only to assess whether the system would be actually technically feasible, but also its economic performances along its lifetime in the light of possible variations in the parameters employed for the modelling.
It is worth it to mention that the choice of end port furnace is suggested by the fact that no existing literature is available on this specific system, and at the same time Bormioli Pharma employs such a furnace, so this could be useful as a reference for a future and potential application of the technology.

6.1. Project's steps and methods

The first step is the realization of the base-model of the existing furnace (no SMR), to be validated against a pre-existing model built up by Bormioli Pharma supplier: this represents the basis on which the SMR unit would be installed.
The second step, once the base-model is validated, is to add the SMR thus obtaining the final system configuration.
The system is designed such that the flue gasses leaving the furnace regenerative chambers provide not only the power required by the endothermic reactions, but also the thermal power needed to supply the mixture of superheated vapour and methane at the thermodynamic conditions at which these reactions are operated. Therefore, exhaust gasses will

[5] Q_{av} is the thermal power of the flue gases between the inlet temperature and the lowest temperature allowable (180°C)

[6] Note that $\eta_{tot} = \eta_{th} \cdot \phi$

first enter the reactor followed by a heat recovery steam generator in parallel with a methane preheating heat exchanger before eventually being sent to the filters.

On the basis of the energetic evaluation of the system, consisting in the exchanged thermal powers, temperatures and flow rates it became possible to size the two main pieces of equipment: the methane preheater and the heat recovery steam generator. The first one has been addressed by means of the *mean logarithmic temperature difference* method, for which a range of the overall heat transfer coefficient has been taken from literature. The **HRSG** instead has been designed by a **Company supplier**, because of its complexity and difficulties in identifying reliable coefficients in literature.

Once the sizing has been accomplished and the most relevant components have been identified, their quotation has been carried out which allows to undertake the economic assessment of the overall system by applying the NPV method. Therefore, cash flows have been computed assuming as incomes the savings from natural gas consumption and carbon emissions which are expected as a result of the SMR.

The applied procedure is run on several cases: first of all, it is of key relevance the ***share of energy*** that the hydrogen within the syngas would replace from natural gas, and different shares have been considered in this regard. Moreover, also the operating conditions of the furnace in terms of ***pull*** and ***electric input*** have been considered as variables, given their relevance on the energy input required. Therefore, a sensitivity analysis is operated on these figures.

Moreover, the economic analysis also includes sensitivity considerations especially for what concerns the ***heat transfer coefficients*** in the heat exchanger design, as well as ***prices of natural gas and carbon emission***.

All the modelling activity is carried out by means of Microsoft Excel.

6.2. Furnace modelling without SMR

The description of the base-model of the existing furnace is taken on.

The domain for the modelling is as in **Figure 12**:

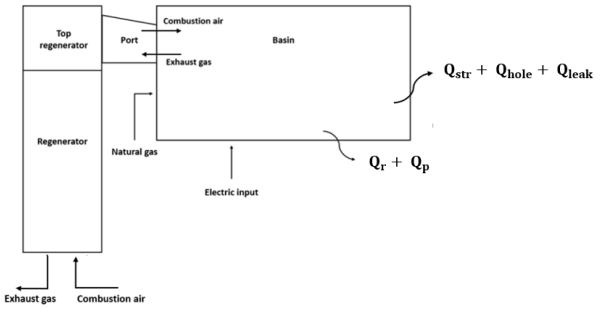

Figure 12 - Furnace base-model domain

The base-model is run at fixed conditions, especially for what concerns *pull* and *cullet*: the first is set equal to the design value, on which the pre-existing model, used as reference for the validation, is tuned. Cullet is also set to the average value both for the base-model and the final configuration[7] (with SMR). For what concerns the *electric input EE,* it is set equal to 0,116 kWh/kg for the validation step.

It is interesting to point out that the **overall heat input Q_{tot}** is taken as a known value: it comes indeed from the analysis of the state-of-art carried out in the previous chapters, more specifically from the assessment of the overall heat demand for each class of furnace (see **Figure 6**). The reference conditions for the energy balances are 298 K and 1 bar.

For sake of simplicity, natural gas is assumed to be composed only by methane.

Table 3 hereinafter provides an insight on the model inputs:

Pull $\left[\frac{ton}{d}\right]$	Q_{tot} $\left[\frac{kWh}{kg}\right]$	Cullet [%]	EE $\left[\frac{kWh}{kg}\right]$	T_{ref} [K]
Design value	1,187	Design value	0,116	298

Table 3 - Inputs and variables for base-model

The furnace heat input is:

$$Q_{tot} = Q_{ee} + Q_{CH_4} \quad [6.\,1]$$

Where the unknown is Q_{CH_4}, from which it is possible to determine the methane flow rate which satisfies the demand:

$$Q_{CH_4}[kW] = \frac{Q_{CH_4}\left[\frac{kWh}{kg}\right] \cdot Pull\left[\frac{kg}{d}\right]}{23^{8}\left[\frac{h}{d}\right]} \quad [6.\,2]$$

$$n_{CH_4}\left[\frac{mol}{s}\right] = \frac{Q_{CH_4}[kW]}{LHV_{CH_4}\left[\frac{J}{mol}\right]} \quad [6.\,3]$$

Mass and energy balances on the furnace are written with the approach of the *extent of reaction* ε_j, where j stands for j-th reaction taking place in the system and i stands for the i-th species[9]:

$$n_{i,\,out}\left[\frac{mol}{s}\right] = n_{i,\,in}\left[\frac{mol}{s}\right] + \sum_{j}^{NR} \nu_{i,j} \cdot \varepsilon_j\left[\frac{mol}{s}\right] \quad [6.\,4]$$

$$\sum_{i}^{n} H_{i,in}[W] = \sum_{i}^{n} H_{i,out}[W] + \sum_{j}^{NR} \varepsilon_j\left[\frac{mol}{s}\right] \cdot \Delta H^{\circ}_{r_j}(T_r)\left[\frac{J}{mol}\right] \quad [6.\,5]$$

The expression of the enthalpy flux can be written by [6. 6]:

$$\sum_{i}^{n} H_i[W] = \sum_{i}^{n} n_i\left[\frac{mol}{s}\right] \cdot \left[h_{i,ref}[W] + \int_{T_{ref}}^{T} C_{p_i}\left[\frac{J}{mol \cdot K}\right] dT\right] \quad [6.\,6]$$

[7] Despite being important, cullet is not taken as a variable in order to simplify the modelling

[8] Because of the switch in the regenerator chambers, burners are stopped for 1 minute at each switch: burners operate 23 h/d

[9] In case of no reaction, such as heat exchange processes, $\varepsilon = 0$

For what regards the $C_{p_i}\left[\frac{J}{mol \cdot K}\right]$, the polynomial relationship [6. 7] was employed to account for temperature dependency:

$$C_{p_i}\left[\frac{J}{mol \cdot K}\right] = R\left[\frac{J}{mol \cdot K}\right] \cdot \left(a_i + b_i \cdot T + c_i \cdot T^2 + \frac{d_i}{T^2}\right) \quad [6.7]$$

The values for the parameters a, b, c and d are taken from reference [8].
The assumption of *complete combustion* is considered, which means that the fuel is entirely reacted: no methane nor carbon monoxide is expected in the exhaust gases. To cope with these simplifying conditions, an air-to-fuel ratio higher than the actual one has been employed which means that combustion is simulated with a greater excess of oxidizer (alfa=11, excess [%] =15,55%).

Finally, the heat balance on the furnace basin can be written as:

$$H_{in} + EE + n_{CH_4} \cdot LHV_{CH_4} = H_{out}(T_{out}) + Q_{s,l,h} + Q_{r,p} \quad [6.8]$$

As external data for the resolution of the heat balance, $Q_{s,l,h} + Q_{r,p}$ are taken from the pre-existent furnace model made available by Bormioli Pharma supplier, which would not be otherwise computable. They are set equal to 49,89% of the overall heat input ($H_{in} + EE + n_{CH_4} \cdot LHV_{CH_4}$).
By setting $T_{in_{air}} = 1300°C$ for the preheated combustion air entering the furnace basin from the port, which is a typical value, the heat balance is solved in the unknown $T_{out_{ex}}$ which represents the temperature of the exhaust gasses leaving the furnace chamber, by exploiting the *goal seek function* available in Excell.
At this point the furnace is characterized in term of temperatures, streams compositions and power fluxes.

Next step is the heat balance on the regenerating chambers, where the only unknown is the outlet temperature of the waste gasses. Therefore, by assuming a heat transfer efficiency for the chambers equal to η_{reg}[10] $= 0{,}95$ and by imposing objective function [6. 9], such a temperature (before the filters) is determined:

$$f_{obj}\left(T_{out_{regenerator}}\right) = \eta_{reg} - \frac{H_{air_{out}} - H_{air_{in}}}{H_{ex_{in}} - H_{ex_{out}}} = 0 \quad [6.9]$$

In order to assess whether the model is valid or not, the *relative percentual error* $err_{rel_{\%}}$ is computed:

$$err_{rel_{\%}} = \left|\frac{x - x_{model}}{x}\right| \quad [6.10]$$

Where x stands for the generic variable from the pre-existing heat balance, whereas x_{model} represents the one computed within this work. If these $err_{rel_{\%}}$ are sufficiently low (<10%), the model is considered to be close to the real system behaviour and therefore it is validated.

In **Table 4** it is possible to observe which are the compared variables as well as the outputs from the current model, together with the corresponding $err_{rel_{\%}}$:

Variable	Pre-existing	Model	$err_{rel_{\%}}$
$H_{in}[kW]$	3.674,42	3.970,85	**8,07**
$H_{out}[kW]$	5.651,16	5.835,38	**3,26**
$T_{out_{ex}}[K]$	1.755,00	1.847,16	**5,25**
$T_{out_{regenerator}}[K]$	761,00	787,36	**3,46**
$\eta_{th}[\%]$	69,14	71,63	**3,61**
$Q_{tot_{furnace}}[kW]$	11.255,81	11.638,18	**3,40**

Table 4 - Model outputs and validation

Noticing that all the errors are well below the 10%, the model is considered validated.

6.3. Furnace modelling with SMR

At this point, it is possible to add the SMR unit to the furnace domain. **Figure 13** represents the process flow diagram of the system:

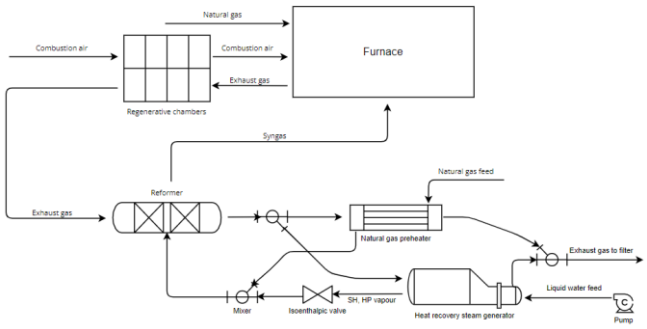

Figure 13 - Process flow diagram furnace + SMR unit

The unit would be placed downstream the regenerator chambers thus exploiting the residual thermal power of the flue gasses, whose temperature must be sufficiently higher than the temperature level set by the chemical equilibrium on the steam reformer which is, as an anticipation, equal to 850K (577 °C) and it represents the temperature at which the steam reforming reactions occur as well as the value at which the syngas leaves the reactor.
The exhaust gases are initially sent to the reformer reactor, where they lose a first amount of thermal power. Secondly, by means of a valve the flow rate is splitted into two different streams of different rates: one is fed to the HRSG where superheated vapor at 20 bar is produced, whereas the other is fed to the methane preheating heat exchanger. These two exhausts flow rates, having the same temperature[11], are then reunited in the downstream mixer before eventually being sent to the filters.
The reforming reactions are operated at the lowest pressure possible of 1 bar, which is why an isoenthalpic valve is present, such that the superheated steam, which can be

[10] How much power get lost (to walls, structure, environment, …)

[11] This is a constraint imposed when computing their flow rates

considered as ideal gas due to the high temperature and moderate pressure, is expanded without reducing neither its enthalpy nor its temperature. The following step is the mixing of vapor and methane, which are now brought at the same thermodynamic conditions (T, p): the resulting mixture is the feed stream which is eventually fed to the reactor.
The reactor output will be syngas at 850 K, which will be burnt into the furnace chamber. It is reasonable to expect that a couple of dedicated burners would be placed approximately at 3/4 of the basin length, one per each side. However, their position and number are not accounted in the thermodynamic simulation.

From the same $\mathbf{Q_{tot}}$ used for the base-model, it is possible to first compute the heat input from combustion:

$$\mathrm{Q_{tot}} = \mathrm{Q_{ee}} + \mathrm{Q_{comb}} \quad [6.\ 11]$$

Where the unknown is $\mathrm{Q_{comb}}$:

$$\mathrm{Q_{comb}[kW]} = \frac{\left(\mathrm{Q_{tot}}\left[\frac{\mathrm{kWh}}{\mathrm{kg}}\right] - \mathrm{EE}\left[\frac{\mathrm{kWh}}{\mathrm{kg}}\right]\right) \cdot \mathrm{Pull}\left[\frac{\mathrm{kg}}{\mathrm{d}}\right]}{23\left[\frac{\mathrm{h}}{\mathrm{d}}\right]} \quad [6.\ 12]$$

At this point, the required thermal power from combustion is determined. The next step is to set the desired share of energy that the hydrogen within the syngas[12] will provide due to its LHV. Then, hydrogen molar flow rate can be computed:

$$\mathrm{n_{H_2}}\left[\frac{\mathrm{mol}}{\mathrm{s}}\right] = \frac{\mathrm{Q_{H_2}[\,kW\,]}}{\mathrm{LHV_{H_2}}\left[\frac{\mathrm{J}}{\mathrm{mol}}\right]} \quad [6.\ 13]$$

The furnace operating conditions are reported in **Table 5**:

Pull	$\mathbf{Q_{ee} + Q_{comb}}$	$\mathbf{Q_{tot}}$	Cullet	EE	$\mathbf{T_{ref}}$
$\frac{\mathbf{ton}}{\mathbf{d}}$	$\frac{\mathbf{kWh}}{\mathbf{kg}}$	[MW]	[%]	$\frac{\mathbf{kWh}}{\mathbf{kg}}$	[K]
135	1,235	10,561			
140	1,222	10,830			
145	1,210	11,099			
150	1,198	11,369	Design value	0,116	298
155	1,187	11,638			
160	1,177	11,907			
165	1,169	12,176			
170	1,160	12,443			

Table 5 - Inputs and variables for furnace + SMR unit model

At this point, the furnace thermal power demand obtained as output from the base-model (also used to validate it) is exploited to compute the methane flow rate that is still required to close the furnace heat balance. In such a way, it is possible to account also for the enthalpy flux associated to the hot streams entering the system (air/syngas):

$$\mathrm{H_{in_{air}}} + \mathrm{EE} + \mathrm{n_{CH_4}} \cdot \mathrm{LHV^{298}{}_{CH_4}} + \mathrm{n_{CH_{4_{syn}}}} \cdot \mathrm{LHV^{850}{}_{CH_4}} + \mathrm{n_{H_2}} \cdot \mathrm{LHV_{H_2}} + \mathrm{n_{CO}} \cdot \mathrm{LHV_{CO}} + \mathrm{H_{in_{syn}}} = \mathrm{H_{out}} + \mathrm{Q_{s,l,h}} + \mathrm{Q_{r,p}} \quad [6.\ 14]$$

Obviously, to compute the flow rate of methane (to be supplied as fuel to the furnace) it must first be solved the chemical equilibrium on the reformer reactor, such that the composition of the syngas as well as the demand of methane and water feed for the SMR can be established.
The **chemical equilibrium** on the reactor consists in computing the equilibrium constants for water gas shift and steam reforming reactions:

$$\begin{cases} \mathrm{K_{eq}}_j^{\,1} = \mathrm{p}^{\sum_i^n \nu_i} \cdot \prod_i^n (\mathrm{y_i})^{\nu_i} \\ \mathrm{K_{eq}}_j^{\,2} = \mathrm{e}^{\left(-\frac{\Delta G^{\circ}_{R_j}(\mathrm{T_{out}})}{\mathrm{R}\cdot \mathrm{T_{out}}}\right)} \end{cases} \quad [6.\ 15]$$

Where *p* is the operating pressure, y_i is the molar fraction of the i-th species in the reactor, $\Delta G^{\circ}_{R_j}(T_{out})$ is the standard Gibbs free energy of reaction j evaluated at the outlet temperature and *R* is the universal gas constant. What is obtained is a system of two equations in two unknowns (molar methane feed x and equilibrium temperature):

$$\mathrm{f_{obj_1}(x, T_{out})} = \frac{\mathrm{K_{eq}}_{\mathrm{SR}}^{\,1}}{\mathrm{K_{eq}}_{\mathrm{SR}}^{\,2}} - 1 = 0 \quad [6.\ 16]$$

$$\mathrm{f_{obj_2}(x, T_{out})} = \frac{\mathrm{K_{eq}}_{\mathrm{WGS}}^{\,1}}{\mathrm{K_{eq}}_{\mathrm{WGS}}^{\,2}} - 1 = 0 \quad [6.\ 17]$$

The outputs are the required methane molar flow rate needed to supply the desired hydrogen molar flow rate and the temperature at the reactor outlet, which is the already mentioned 850 K.

At this point, via **heat balance on furnace** it is possible to compute the natural gas demand:

$$\mathrm{f_{obj_3}(n_{CH_4})} = \mathrm{Q_{tot}} - \left(\mathrm{H_{in_{air}}} + \mathrm{H_{in_{syn}}} + \mathrm{EE} + \mathrm{n_{CH_4}} \cdot \mathrm{LHV^{298}{}_{CH_4}} + \mathrm{n_{CH_4}} \cdot \mathrm{LHV^{850}{}_{CH_4}} + \mathrm{n_{H_2}} \cdot \mathrm{LHV_{H_2}} + \mathrm{n_{CO}} \cdot \mathrm{LHV_{CO}}\right) = 0 \quad [6.\ 18]$$

The free variable that can be tuned at each simulation is on the temperature of the preheated combustion air $\mathrm{T_{in_{air}}}$. At normal operating conditions, it is equal to 1300°C. However, such a level of temperature might not be achievable because of the SMR unit presence downstream the regenerator. Indeed, the higher $\mathrm{T_{in_{air}}}$ the better is the heat recovery taking place within the regenerative chambers. As a consequence

[12] LHV of syngas is not known as it depends on its composition, which varies from simulation to simulation

then, the waste gasses leaving the chamber would be well cooled down (in traditional end port furnaces they are in the range 450-500°C). The fact that the SMR unit is placed downstream means that flue gases must be at a temperature sufficiently higher than 850 K (577 °C): as a reference value, such a difference between these two temperatures is chosen to be higher than 20°C. Therefore, $T_{in_{air}}$must be set accordingly and it is only acceptable if the above condition is respected, which is something to be checked after the heat balance on the regenerator. Hence, a trade-off between heat recovery in the chambers and in the SMR unit is to be sought.

At this point, all the flow rates are fully determined, and it is possible to set the heat balance on the furnace whose unknown is the waste gasses outlet temperature from the basin. It can be computed with objective function [6. 19]:

$$f_{obj_4}(T_{out_{ex}}) = H_{in_{air}} + EE + n_{CH_4} LHV^{298}{}_{CH_4} + n_{CH_4{}_{syn}} LHV^{850}{}_{CH_4} + n_{H_2} LHV_{H_2} + n_{CO} LHV_{CO} + H_{in_{syn}} - H_{out} - Q_{s,l,h} - Q_{r,p} = 0 \quad [6.\ 19]$$

The following step consists in performing the heat balance on the **regenerator chambers** to compute the waste gasses outlet temperature:

$$f_{obj_5}\left(T_{out_{reg}}\right) = \eta_{reg} - \frac{H_{air_{out}} - H_{air_{in}}}{H_{ex_{in}} - H_{ex_{out}}} = 0 \quad [6.\ 20]$$

It is at this step that it is possible to state whether the above-set value of $T_{in_{air}}$is compatible with the constraint on the temperature difference between exhausts gases and chemical equilibrium (850 K):

$$T_{in_{air}} \text{ acceptable if } \quad \Delta T = T_{out_{reg}} - 850\ K > 20$$

$$T_{in_{air}} \text{ not acceptable if } \quad \Delta T = T_{out_{reg}} - 850\ K < 20$$

If not, a new and lower $T_{in_{air}}$would need to be imposed and the procedure would restart from the resolution of $f_{obj_3}(n_{CH_4})$.
Then, the modelling of the SMR unit is pursued. At this level of accuracy, no distinction is made between methane heat exchanger and HRSG: these are initially modelled as a unique box (**Figure 14**), as the target of the step is to fully determine the thermodynamic quantities of the involved streams (temperatures, thermal powers):

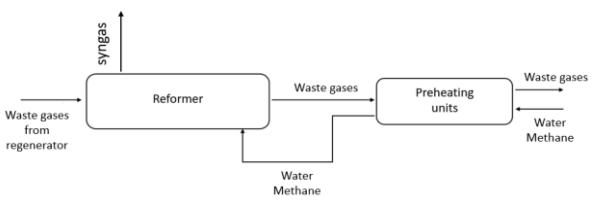

Figure 14 - SMR unit

The unknown variables in such a domain are two temperatures, both on waste gases side: the intermediate one (between reactor and preheating unit) and at the system outlet (lowest thermal level for the entire system).
These can be computed by setting the two objective functions [6. 21][6. 22] to be solved in series (heat balances on reactor and preheating units):

$$f_{obj_6}(T_{ex}) = H_{ex}^{in} + H_{w,m} - H_{ex}(T_{ex}) - H_{syn} - \varepsilon_{SR} \cdot \Delta H^0_{R_{SR}}(850\ K) - \varepsilon_{WGS} \cdot \Delta H^0_{R_{WGS}}(850\ K) - n_{CH_4} R \int_{T_{in_r}}^{850} C_p dT - n_{H_2O} R \int_{T_{in_r}}^{850} C_p dT = 0 \quad [6.\ 21]$$

$$f_{obj_7}\left(T_{ex}{}^{out}\right) = H_{ex} + H_{w,m}^{in} - H_{ex}^{out}\left(T_{ex}{}^{out}\right) - H_{w,m} = 0 \quad [6.\ 22]$$

From f_{obj_6} the intermediate temperature is computable, from f_{obj_7} the waste gases outlet temperature.

Once these two temperature levels are established, it is possible to split the control volume representing the HRSG and methane preheater, which operate in parallel, in order to characterize their thermodynamic features in terms of flow rates (waste gasses side) and exchanged thermal powers.
To compute the molar flow rates, the following assumptions were made:

- The waste gasses flow rate leaving the reactor is not equally splitted among HRSG and methane preheater, however their molar composition is fixed
- Superheated vapor and methane feeds reach the same outlet temperature of 490 °C
- The two waste gasses flow rates at HRSG and methane preheater outlet are at the same temperature $T_{ex}{}^{out}$

Hence, the two flow rates have been computed by setting a heat balance on HRSG [6. 23] and methane preheater [6. 24]:

$$n_{ex}^{HRSG} = \frac{n_{H_2O} \cdot \left[C_{p_{liq}}^{H_2O} \cdot (T_{evap} - 298) + \Delta H_{evap} + R \int_{T_{evap}}^{490} C_{p_{vap}} dt\right]}{\sum_i^n y_i \cdot C_{p_i} \cdot \left(T_{ex} - T_{ex}{}^{out}\right)} \quad [6.\ 23]$$

$$n_{ex}^{meth.PH} = \frac{n_{CH_4} \cdot R \int_{25}^{490} C_p dt}{\sum_i^n y_i \cdot C_{p_i} \cdot \left(T_{ex} - T_{ex}{}^{out}\right)} = n_{ex} - n_{ex}^{HRSG} \quad [6.\ 24]$$

This allows to compute the thermal powers exchanged in the HRSG and methane preheater, as the temperature levels are all known at this point.
From the exhaust gasses side instead, temperatures T_1(economizer inlet) and T_2 (superheater outlet) need to be computed to fully characterize the waste gases side ($T_2 > T_1$) which is done by applying the two objective functions [6. 25],[6. 26] representative of the heat balances on economizer and evaporator:

$$f_{obj_8}(T_1) = Q_{eco} - (H_{ex}(T_1) - H_{ex}^{out}) = 0 \quad [6.\ 25]$$

$$f_{obj_9}(T_2) = Q_{evap} - \left(H_{ex}(T_2) - H_{ex}(T_1)\right) = 0 \quad [6.\ 26]$$

This closes the section related to the thermodynamic modelling of the system.
Figure 15 represents the **schematized resolution procedure**:

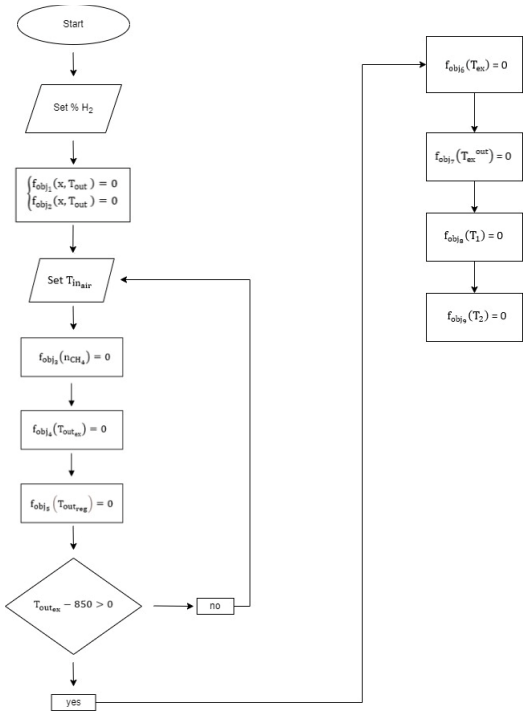

Figure 15 - Procedure block flow diagram

6.4. Methane preheater sizing

This is accomplished by applying the approach of the *logarithmic mean temperature difference:*

$$Q_{CH_4}[\,W\,] = U\left[\frac{W}{m^2K}\right] \cdot A[\,m^2\,] \cdot \Delta T_{ml}[\,K\,] \qquad [6.\,27]$$

Where *U* is the *overall heat transfer coefficient* and *A* is the *surface of heat exchange* on waste gasses side. According with literature [9], [10] typical values of U for gas-gas heat exchangers are in the range $[5, 40]\ \frac{W}{m^2K}$. To account for the uncertainty on U, a sensitivity analysis is carried out by taking first 5 and then 40 such that a reliable esteem on the likely range for A is provided.

6.5. HRSG

The design of the steam generator has been carried out by a Company supplier, on the basis of the outcomes obtained from the thermodynamic modelling (flow rates, exchanged thermal power, temperatures). Initially, the idea was to set up the unit consisting of economizer, evaporator and superheater with water inlet at 20 bar and 25°C (reference temperature) and vapour outlet at same 20 bar and temperature as close as possible to the 850 K. However, following up a discussion with the supplier, it has been decided to apply two changes:

1. Water at the unit inlet (25°C) is first pumped to 4 bar and then preheated with a flow rate of superheated vapour, which is bled at the outlet conditions, to about 120 °C. At these conditions (subcooled liquid), water is fed to a deaerator where the volatile species are extracted. This avoids the condensation of SO_2, which at 20 bar and low temperature is below the dew-point curve[13]. Water is then pumped to 20 bars

2. The outlet temperature of superheated steam is relevant not only for the thermodynamic of the process, but also for the choice of the metals of the superheater. It is suggested a maximum outlet temperature of 490 °C which would allow to operate safely with a commercial steel P22. For higher temperatures instead, more peculiar metals should be employed.

Moreover, according with the designer, because of the important amount of dust in the flue gases, it was not possible to adopt finned surfaces which would have made it possible to reduce quite significantly the heat transfer area.

6.6. Results and sensitivity

The idea is to analyse separately the outcomes: first will be proposed the potential savings, with respect to the base-model, in terms of CH_4 and CO_2 , together with the sensitivity analysis on pull and electric input. The goal is not only to identify whether all the $\%H_2$ are able to bring to satisfactory savings, but also to establish at which percentage the highest performance is obtained, and if this is really achievable or technological limitations exist. Savings are defined as:

- $\Delta CH_4\left[\frac{sm^3}{y}\right] = \left(V_{CH_4}^{SMR} - V_{CH_4}^{no\ SMR}\right)$
- $\Delta CO_2\left[\frac{ton CO_2}{y}\right] = \left(m_{CO_2}^{SMR} - m_{CO_2}^{no\ SMR}\right)$

For the case of **fixed electric input (0,116 kWh/kg)** and **variable pull**, the results are plotted (in percentual terms). Note that three levels of pull are taken, indicated as lower, middle and higher:

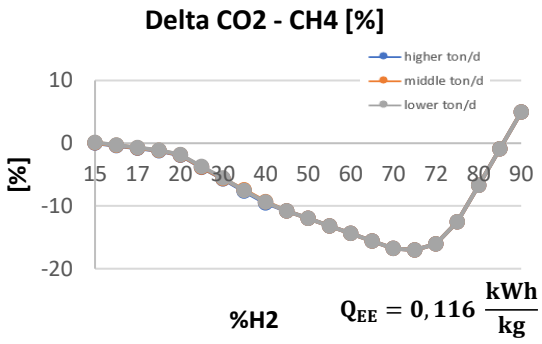

Figure 16 - Savings in carbon emission against pull [%]

Instead, for the case of **variable electric input between 0,070, 0,093 and 0,116 kWh/kg** and **fixed pull** at middle ton/d:

[13] Sulphur oxide would condensate and react with water into sulphurous acid, highly corrosive for common metals

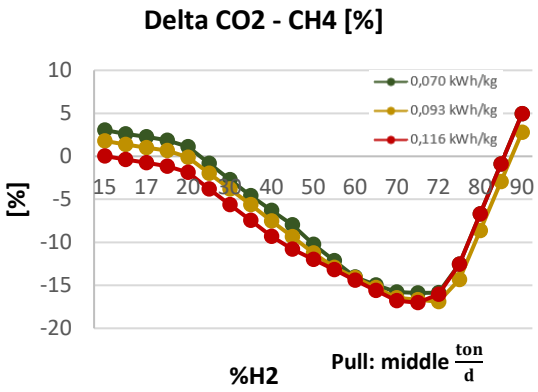

Figure 17 - Savings in carbon emissions against ee [%]

What can be noticed is that a non-monotonic behaviour of both CH_4 and CO_2 is expected. A beneficial effect of the system is for $\%H_2$ between 16 and 85 with a point of maximum in the range 65-75%. Moreover, stronger differences are to be expected when electric input varies rather than the pull, hence it can be stated that the model has a limited sensibility on pull variations but stronger on electric input.

However, the last question is yet to be addressed: are there any technological limitations on the possibility to adopt such high shares? From a thermodynamic perspective, the main limitation is coming from the temperature at which the exhaust gases would leave the system ($T_{ex}{}^{out}$), before being sent to the filter. It is indeed the presence of the filter the major limitation, since it is the component that sets the flue gases lowest temperature within the process and, therefore, the heat recovery that can be achieved by the system. According with the type of filter, these are the limiting temperatures:

- Electrostatic filter: T=280 °C
- Baghouse filter: T=180 °C

If these technological constraints were imposed, it would follow that it might not be possible to achieve those 65-75% able to optimize the system. It is possible to state that the optimum conditions become:

- 40-45 $\%H_2$, for electrostatic filter
- 55-60 $\%H_2$ for baghouse filter

6.7. Heat exchanger sizing

The heat exchanger sensitivity analysis on the variable U is also taken on (between 5 and 40 $\frac{W}{m^2K}$) together with the effect of pull and electric input.

The **first plot** shows the surface dependency on pull and U at **fixed electric input**, whereas the **second** is about electric input and U a **fixed pull**.

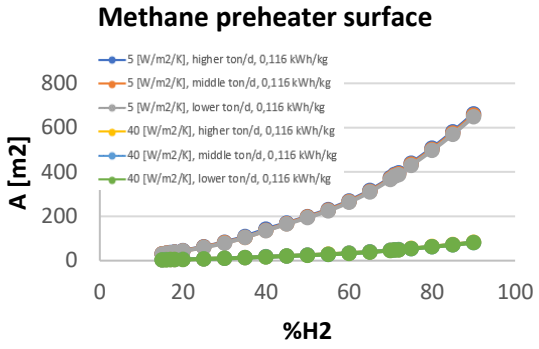

Figure 18 - Methane preheater surface against U, pull at fixed ee

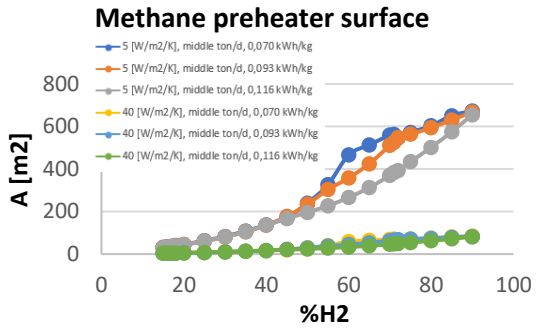

Figure 19 - Methane preheater surface against U, ee at fixed pull

Results tell that U is definitely a major variable that must be considered, as strong differences are to be expected when it undergoes significant changes. It appears that, ranging from 5 to 40 $\frac{W}{m^2K}$, the surface increases 8 times: this shall not be unexpected, given the linearity of the mean logarithmic temperature difference approach with respect to U.

6.8. Equipment quotation

The cost of each piece of equipment has been estimated, taking into account also the sensitivity analysis performed. The components addressed are:

- Reforming reactor
- Methane preheater
- HRSG
- Couple of additional burners

For the case of the ***reforming reactor***, the approach consisted in searching for a reference [11] able to tell the cost associated with its hydrogen mass flow rate production. Then, the correlation [6. 28] is exploited:

$$\frac{C_a}{C_b} = \left(\frac{A_a}{A_b}\right)^n \qquad [6.\ 28]$$

Where C_a, C_b represent the costs while A_a, A_b are the equipment cost attributes (hydrogen output in kg/h) and n=0,6 is an exponent which accounts for the non-linear relationship, which can also be accounted as for an "economy of scale".

Once again, the results of the cost estimation are analysed by taking into account different pulls and electric inputs.
Figure 20 summarizes the reactor expected quotations:

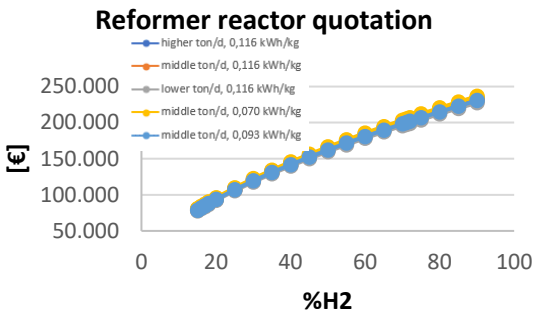

Figure 20 - Reformer reactor quotation against pull and ee

Almost overlapped curves indicate that the expected cost is basically independent of the two variables.

For what regards the ***methane preheater***, once the size has been established it is a matter of applying a reliable correlation for the quotation.
By applying the Turton's correlation [12] and by **varying pull** and **electric input** on the two different values of U (5 and 40 $\frac{W}{m^2K}$):

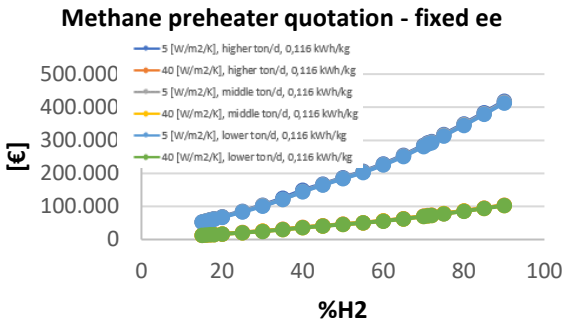

Figure 21 - Methane preheater quotation against U, pull at fixed ee

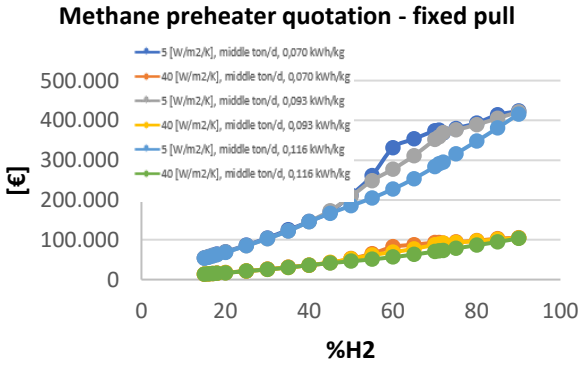

Figure 22 - Methane preheater quotation against U, ee at fixed pull

For what regards the quotation of the ***HRSG***, as anticipated it is provided by a supplier together with its design and sizing. The offer includes also the circulation and feed pumps, valves and instrumentation, insulation, electric panel and certification H72[14]. The budgetary proposal for the overall set is 415.000€.
Even though the design was specifically carried out for the solution at 40% of hydrogen share (what would change from case to case would be the involved thermal powers and flow rates), according with the designer of the supplying company there were only slight differences with the other configurations in terms of equipment size and quotation. Therefore, this solution is taken as reference for the HRSG quotation.

Last, for the case of ***burners***, the cost indication comes from a Company supplier. Accordingly, the offer would include a set of two burners, dedicated supports, brackets and pressure gauges. The overall cost would be around 20.000-25.000 €. Moreover, it is suggested a replacement of each burner every three years, which is to be accounted in the cash flow calculation.

6.9. Economic analysis

The approach of the Net Present Value has been applied in order to take into account the time value of money along the lifetime of the project, which is as long as a furnace campaign.

$$NPV = \sum_{t=1}^{N} \frac{F_t}{(1+i)^t} - F_0 \qquad [6.\ 29]$$

For what regards the positive cash flow, the CH_4 and CO_2 savings with respect to the base-model are considered (furnace without SMR unit). The main uncertainty here is about their prices, which are strongly fluctuating and steadily on a rising path. To smooth down such an unpredictability, a sensitivity analysis is operated.

This analysis seeks at establishing whether the project is actually feasible in economic terms and which configuration (% H_2) would achieve the highest performance. Similarly to what done in the previous sections, a sensitivity analysis is carried out on the following variables: ***pull, electric input, overall heat transfer coefficient U, price of methane*** and ***price of carbon emission***.
The approach is summarized in the chart:

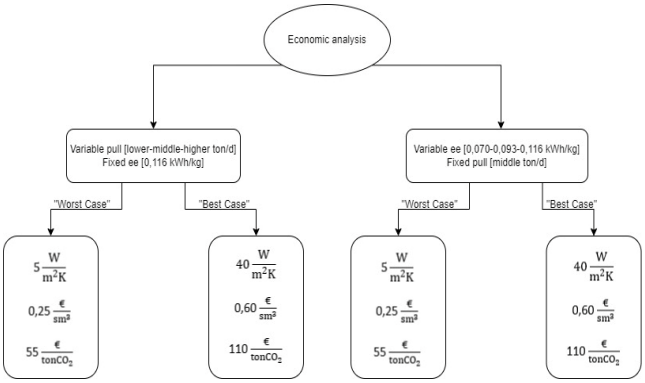

Figure 23 - Sensitivity structure for economic analysis

[14] Specific certification for pressurized steam generator from waste gasses comprising a number of equipment and instrumentation

Where "worst case" and "best case" represent the scenarios in which the project would appear the least[15] and the most[16] profitable, respectively.
This should allow on the one hand to establish the influence of pull and electric input, on the other to define the range where the actual NPV should be located for any value of U and methane/carbon prices, as long as these are between 5 and 40 $\frac{W}{m^2K}$, 0,25 and 0,60 $\frac{€}{sm^3}$, 55 and 110 $\frac{€}{tonCO_2}$ respectively. Once the calculations have been carried out, the results have been collected and plotted. The output is, for each of the twelve cases, the corresponding NPV for each hydrogen share, which is made varying between 15 and 60 %, the latter being the ultimate technologically feasible configuration:

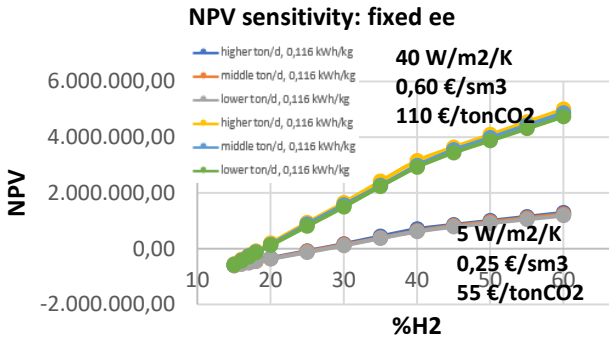

Figure 24 - NPV sensitivity at fixed electric input

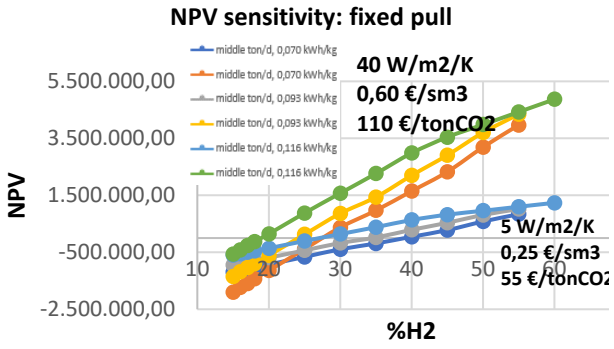

Figure 25 - NPV sensitivity at fixed pull

The analysis brings to the conclusion that the NPV at the optimal operating conditions is expected within the ranges:

- Electrostatic filter 40% H_2: 44.824 < NPV [€] < 3.150.312
- Baghouse filter 60% H_2: 837.288 < NPV [€] < 4.997.349

To conclude, in on design conditions the system would be able to provide rather interesting performances both from the CH_4/CO_2 and economic viewpoints. Indeed, in case of **electrostatic filter**, up to **10% of CH_4/CO_2 savings** together with a NPV in the range **44.824 and 3.150.312 €.** For the case of **baghouse filter** instead, more ambitious numbers can potentially be pursued such as a **15% cut in CH_4/CO_2** and NPV of **837.288 to 4.997.349 €**.

7. Conclusions

The goal of the Thesis is to address the challenge of decarbonization of the glass industry, which is doubtlessly an energy intensive sector. In doing so, it is fundamental to first analyse the state-of-art of the energy demand and carbon emissions associated with the actual furnaces. By exploiting the data made available by the Company, it was possible to design a method, based on energy balances, which enables to compute the theoretical specific energy demand $\left[\frac{kWh}{kg}\right]$ as a function of the three most important independent variables: **pull**, **cullet** and **electric input**. This, coupled with the *energy efficiency index* which accounts for the ageing of the furnace, allows to have a picture of the overall theoretical specific energy consumption (and emissions) of the given furnace along its lifetime. From the index it can be noted that typical values of increase are +40/50% for electric, +50/60% for Cyclope and +30/35% for end port and unit melter furnaces.
For what regards the furnace comparisons accomplished in chapter 3, for the case of soda-lime **Figure 6** shows that end-port is less energy demanding than unit melter, at same conditions. This is expected, considering that end port is basically the development of the unit melter thanks to its enhanced heat recovery capability. For the borosilicate instead, **Figure 5** suggests that electric furnaces have a much better thermal efficiency than Cyclope thus leading to a lower energy demand, considering that the mechanism of heat transfer is more effective and that no exhaust gases are present. However, chapter 3 also wants to discuss the reasons why fired-based furnaces are still preferred: from the point of view of the operating costs (electricity, fuel, CO_2) the analysis highlights the fact that up until the recent past the economic conditions in terms of electricity/natural gas/carbon allowances were not fit yet for an overcome of the full electric over the hybrid.

Chapter 5 deals with the waste heat recovery – heat to power approach introduced in chapter 4. It is based on an existing paper [7] that analyses the implementation of four different thermodynamic cycles for the heat recovery from waste gases downstream an end port furnace operating at 150 ton/d, which is a close case to the actual operating conditions of interest. This is a rather suitable case study for Bormioli Pharma too because it analyses the feasibility in terms of potential power output from these systems as well as their economic performances. The goal of the authors is to determine whether alternative cycles to the well-established and market-ready ORC are actually more competitive. Even though the *Closed loop, sCO_2 JB cycle with combustion air preheating* can potentially achieve the best net power output of 473,3 kW, authors claim that *ORC* is still ahead in terms of economic performances: ROI between 6 and 7,5 years and net power output of 359 kW.

The last section of the Thesis, chapter 6, provides the thermodynamic and economic model of the steam methane reforming unit applied to an end port glass furnace. The

[15] Low U means bigger surface and therefore higher cost, combined with the lowest methane and carbon dioxide savings

[16] high U means smaller surface and therefore lower cost, combined with the highest methane and carbon dioxide savings

purpose is to evaluate the technical feasibility in on design operations in terms of fuel and carbon emission savings with respect to the system without SMR unit. The project is then completed with a sizing of the main equipment, their quotation as well as an economic evaluation of the project performances in terms of Net Present Value. Moreover, a sensitivity analysis is operated on the most relevant design and operating variables among which there are hydrogen energetic input, pull, electric input, overall heat transfer coefficient for the methane preheater sizing and CH_4/CO_2 prices.

The model shows very promising results, both from fuel/emissions savings and economic feasibility: in case of electrostatic filter, up to 10% of CH_4/CO_2 savings together with a NPV in the range 44.824 and 3.150.312 €. For the case of baghouse filter instead, more ambitious numbers can potentially be pursued such as a 15% cut in CH_4/CO_2 and NPV of 837.288 to 4.997.349 €. Hence, the project is not only judged as technically feasible, but also economically convenient with respect to the standard end port furnace.

Lastly, it is believed that such an approach of heat recovery, based on the exploitation of thermal energy finalised at the direct production of heat, would be the most performing way. Going through the conversion of flue gases thermal content into mechanical first and electrical then is indeed associated with an outstanding loss of energy. Unfortunately, steam reforming applied to glass furnaces is not yet developed and therefore not ready for a market deployment. Tests and pilot projects are under development: hopefully, this technology will succeed in making its entry in the glass sector giving its contribution for a more sustainable glass production.

List of figures

List of tables

Bibliography

[1] ARERA, [Online]. Available: https://www.arera.it/it/dati/gpcfr2.htm.

[2] ARERA, [Online]. Available: https://www.arera.it/it/dati/eepcfr2.htm.

[3] SANDECO2, [Online]. Available: https://www.sendeco2.com/it/prezzi-co2.

[4] Life Sugar Project, [Online]. Available: https://www.lifesugarproject.com/.

[5] M. Fiehl, J. Leicher, A. Giese, K. Gorner, B. Fleischmann e S. Spielmann, «Biogas as a co-firing fuel in thermal processing industries: implementation in a glass melting furnace,» 2017.

[6] NSG Group, [Online]. Available: https://www.nsg.com/en/media/ir-updates/announcements-2021/ag-production-powered-by-hydrogen.

[7] P. Danieli, S. Rech e A. Lazzaretto, «Supercritical CO2 and air Brayton-Joule versus ORC systems for heat recovery from glass furnaces: Performance and economic evaluation,» 2018.

[8] H. C. van Ness, J. M. Smith e M. M. Abbott, Introduction to Chemical Engineering Thermodynamics, New York: McGraw-Hill, 1996.

[9] Y. A. çengel, Termodinamica e trasmissione del calore, McGraw - Hill Companies srl, 2009.

[10] «The Engineering Toolbox,» [Online]. Available: https://www.engineeringtoolbox.com/heat-transfer-coefficients-exchangers-d_450.html.

[11] National Renewable Energy Laboratory, «Equipment Design and Cost Estimation for Small Modular Biomass Systems, Synthesis Gas Cleanup, and Oxygen Separation Equipment; Task 1: Cost Estimates of Small Modular Systems,» 2006.

[12] O. J. Symister, «An Analysis of Capital Cost Estimation Techniques for Chemical Processing,» 2016.

Nomenclature & symbols

NOMENCLATURE	SYMBOLS
EE – ELETRIC ENERGY	ΔT_{ml} **[K]** – logarithmic mean temperature difference
EEI – ENERGY EFFICIENCY INDEX	Q_{ee} **[W]** – electric heat input
HRS – HEAT RECOVERY SYSTEM	Q_{ex} **[W]** – exhaust gasses heat flux
HRSG – HEAT RECOVERY STEAM GENERETOR	Q_{ng} **[W]** – natural gas heat input
JB – JOULE BRAYTON	$Q_{r,p}$ **[W]** – heat flow due to reactions and glass leaving the furnace
LHV – LOWER HEATING VALUE	$Q_{s,l,h}$ **[W]** – heat leakage due to structure, leakage, holes
NPV – NET PRESENT VALUE	$\varepsilon_j \left[\frac{mol}{s}\right]$ – extent of reaction j
ORC – ORGANIC RANKINE CYCLE	$\nu_{i,j}$ – stoichiometric coefficient of species i in reaction j
ROI – RETURN ON INVESTMENT	$\Delta G^{\circ}_{R_j}(T)$ – Standard Gibbs free energy of reaction j evaluated at temperature T
SMR – STEAM METHANE REFORMING	$C_{p_i} \left[\frac{J}{mol \cdot K}\right]$ – Specific heat at constant pressure
$\Delta CH_4 \left[\frac{sm^3}{y}\right]$ – METHANE SAVINGS	$\Delta H^{\circ}_{r_j}(T) \left[\frac{J}{mol}\right]$ - Standard heat of reaction j at temperature T
$\Delta CO_2 \left[\frac{ton CO_2}{y}\right]$ – CARBON EMISSION SAVNGS	F_t – Cash flow at year t
	$K_{eq,j}$ - Equilibrium constant for reaction j